Updates on the Fixed Threshold Mixing Model

Mari Kawakatsu and Christopher K. Tokita

Last updated: March 4, 2019

Contents

1 Summary

In our previous theoretical investigation, we had found the following results:

- Varying the task performance efficiency (α) by ant type produced different average task performance frequencies in the pure colonies, analogous to the different mean RMSD values observed empirically.
- Varying α also produced patterns of behavioral contagion in the mixed colonies, including some asymmetry in the direction of contagion (but also see point 1 below).
- Somewhat counterintuitively, varying only the mean threshold (μ) by ant type did not produce different average task performance levels in the pure colonies, although it did produce behavioral "amplification" (i.e. greater behavioral specialization) in the mixed colonies.

Over the past weeks, we used both computational simulations (Sections 2-4) and analytical calculations (Section 5) to address the questions identified in our previous discussions. Our key findings are as follows:

1. Asymmetries in behavioral contagion with genetic mixing

   (a) **Pure and 50:50 mixes**: In the genetic mixing experiments (Fig. 1 in Yuko's summary), the data show different asymmetries in behavioral contagion depending on the type of larvae: we have previously discussed how the contagion can be characterized as "upward" in GEN1 and as "downward" in GEN2.[1] We wanted to understand **how the FTM could reproduce these different asymmetries resulting from the interaction between the larvae and ant types**. To do so, we varied the task demand rate (δ) associated with each task—as a proxy for different larvae type—in addition to varying the task performance efficiency (α)—as a proxy for ant type.

   - When both lines are efficient[2], we only observed **downward contagions**. Changing the demand rate had no qualitative effect (Fig. 1 below).[3]
   - When one line is efficient and the other is inefficient, we only observe **upward contagions**. Changing the demand rate had no qualitative effect (Fig. 2 below).
   - When one line is efficient and the other is efficient or inefficient depending on the demand rate, we observe **both upward and downward contagions**. Changing the demand rate has a nontrivial qualitative effect (Fig. 3 below).

   (b) **Non-50:50 mixes**: So far we focused on comparing pure colonies or 50:50 mixes. To further investigate how well the FTM explains the dynamics of mixed colonies, we studied the effect of varying the ratios of A and B ants on task performance (in this analysis we vary only α and keep δ fixed). Both simulations (Figs. 4 and 5) and analytical calculations (Section 5.3) predict that the **colony-level mean task performance changes nonlinearly as the mix ratio is varied**.

2. Lack of behavioral contagion with demographic and morphological mixing

   - In the demograpic and morphological mixing experiments (Figs. 2 & 3 in Yuko's summary), the data show that the ant types differ in behavior but the behavior of each type is unaffected by mixing. We wanted to understand how the FTM could capture these observed patterns. We found that **varying the task efficiency (α) and either the mean threshold (μ) or the threshold variance (σ) by ant type could capture these "negative" results** (Figs. 6 & 7 below).

Based on our findings, we have several questions for you:

- **Are both lines feasible long-term individually and in the genetic mixes**? If not, **which genetic line is dominant**? We are interested in this because both our simulations and analytical predictions suggest that whether the colony demands can be met makes a significant difference. *(We look forward to continuing our ongoing discussion on these questions and learning the results of the dissections.)*
- **Would it be possible to run additional experiments with different mixes?**
- **What are the biological interpretations of the presence and absence of behavioral contagions as well as the directions of contagion (upward vs. downward)**? We have found that, at least in some cases, multiple parameter combinations can give rise to similar patterns. Knowing the biological story would help us narrow down the most plausible mechanisms.

[1] We use "upward" (respectively "downward") contagion when the mean task performance of the mixed colonies is higher (respectively lower) than the mean task performance of the pure colonies. See Fig. 11 for a schematic.

[2] We use "efficient" to mean that ants are able to meet the demand for both tasks (i.e., stimuli maintain a steady value on average over time) and "inefficient" to mean that the ants are unable to do so (i.e., stimuli keep increasing over time). Holding all other parameters fixed, efficiency is determined by an interaction between the task demand rate and the task performance efficiency.

[3] We were able to show analytically that, if both lines are efficient, then **only downward contagions are possible** under any combination of demand rate (δ) and task efficiency (α), all other parameters being equal.

2 Varying task demand rate and task efficiency

To capture the effects of larval type on task performance, we varied the task demand rate (δ) in addition to the task performance efficiency (α). In particular, we were interested in whether this combination could give rise to the different directions of contagion (upward or downward) observed in the data. For simplicity, these simulations assumed that both tasks associated with a given type of larvae (A or B) have the same demand rate (i.e. $\delta_1 = \delta_2 = \delta$).

We first consider the case in which both lines are efficient and, for a given value of δ, line B is more efficient than line A (Fig. 1). In this case, the ants in the pure-B colonies are less active than those in the pure-A colonies; in the mixed colonies, we observe downward contagions. Changing the demand rate makes no qualitative difference in this relative ordering.

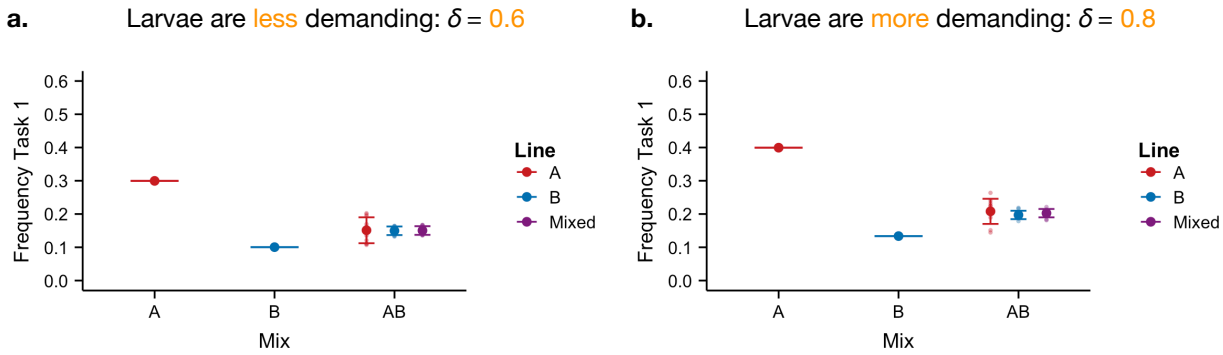

Figure 1: Simulation results for varying both the demand rate (δ) and the task efficiency (α). For a fixed δ, line B is more efficient than line A. **a**: Larvae are less demanding ($\delta = 0.6$). **b**: Larvae are more demanding ($\delta = 0.8$). Parameters: $\alpha_j^A = 2$, $\alpha_j^B = 6$, $\sigma = 0.1$, $\mu = 10$, $\eta = 7$.

Next we explore the scenario where one line is efficient (line A) and the other is inefficient (line B); we consider two larval lines (i.e. two values of δ) that maintain this relationship (Fig. 2). In this case, the ants in the pure-B colonies are more active than those in the pure-A colonies; in the mixed colonies, we observe upward contagions. Changing the demand rate makes no qualitative difference in this relative ordering. Note that the task performance level for the inefficient pure-B colonies does not change when δ changes. This happens because the inefficient B ants—which, by definition (see Summary), are unable to meet the colony demands—end up working at maximum capacity in both cases.

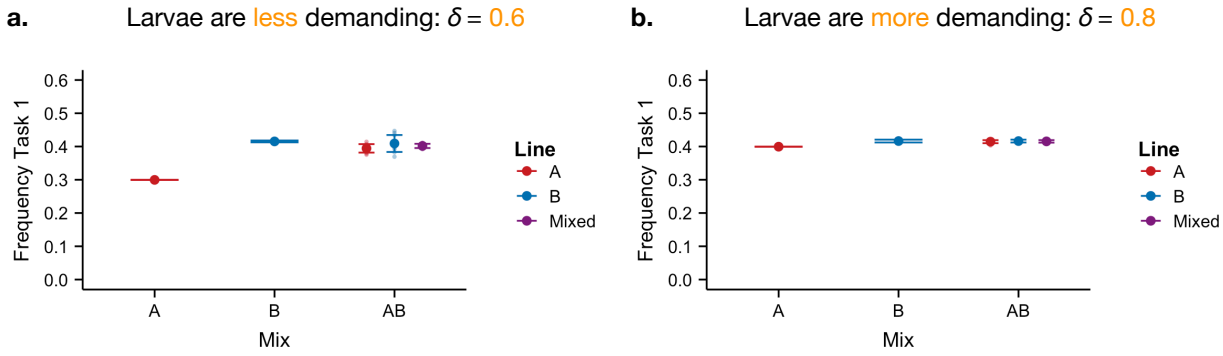

Figure 2: Simulation results for varying both the demand rate (δ) and the task efficiency (α). For both values of δ, line A is efficient while line B is inefficient. **a**: Larvae are less demanding ($\delta = 0.6$). **b**: Larvae are more demanding ($\delta = 0.8$). Parameters: $\alpha_j^A = 2$, $\alpha_j^B = 1$, $\sigma = 0.1$, $\mu = 10$, $\eta = 7$.

Finally, we study the case in which varying the demand rate (δ) alters the direction of contagion. Here we consider two larval lines (i.e. two values of δ) such that one genetic line (line B) is efficient for one larval type but inefficient for the other; the other genetic line (line A) is efficient for both larval types (Fig. 3). When the larvae are less demanding (Fig. 3**a**), both lines are efficient; in this case, we observe a downward contagion in the mixes, similar to Fig. 1. On the other hand, when the larvae are more demanding (Fig. 3**b**), line A remains efficient but line B becomes inefficient; in this case, we observe an upward contagion in the mixes, similar to Fig. 2. In this way, changing the demand rate can alter the contagion pattern qualitatively when one of the genetic lines changes from being efficient to being inefficient.

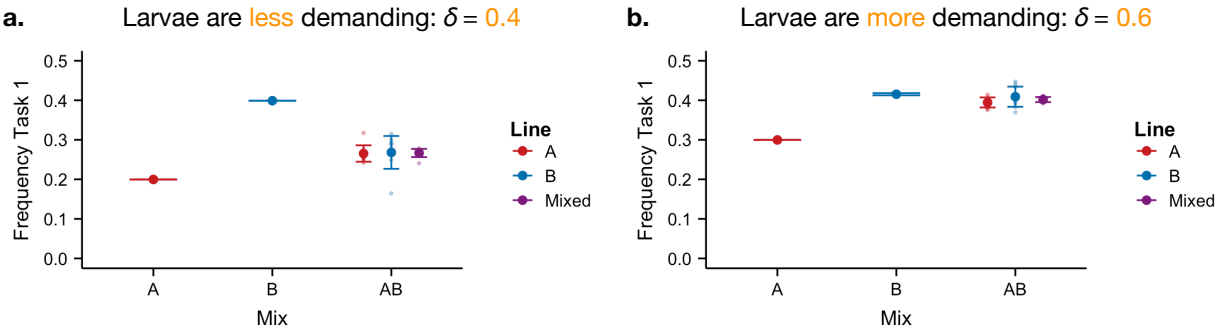

Figure 3: Simulation results for varying both the demand rate (δ) and the task efficiency (α). **a**: Larvae are less demanding . **b**: Larvae are more demanding ($\delta = 0.6$). For a given δ, line A is more efficient than line B. Line B is efficient when the larvae are less demanding (**a**) but inefficient when the larvae are more demanding (**b**); line A is efficient in both cases. Parameters: $\alpha_j^A = 2$, $\alpha_j^B = 1$, $\sigma = 0.1$, $\mu = 10$, $\eta = 7$.

3 Varying ratios of the genetic lines

Increasing the number of mix ratios demonstrates a non-linear effect with regard to task performance. When exploring these mixes, we held genetic line A as efficient ($\alpha_j^A = 2$) and varied the task efficiency of genetic line B. The larval type was fixed ($\delta = 0.6$). When B is more efficient than A ($\alpha_j^B = 6$, Fig. 4), the frequency of task 1 performance increases nonlinearly as the proportion of line A increases. On the other hand, when B is inefficient ($\alpha_j^B = 1$, Fig. 5), task 1 performance decreases nonlinearly as the proportion of A increases. Overall, this predicts that experiments with more mixing ratios will show a nonlinear trend, assuming that task efficiency is the only difference between the two lines.

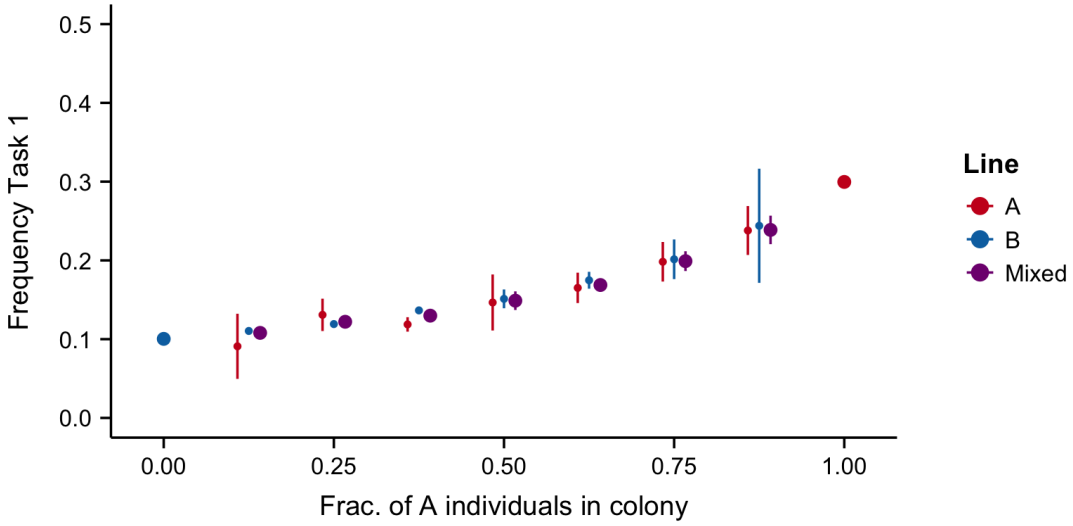

Figure 4: Simulation results for mixing of genetic lines when line B is efficient. Parameters: $\alpha_j^A = 2, \alpha_j^B = 6$.

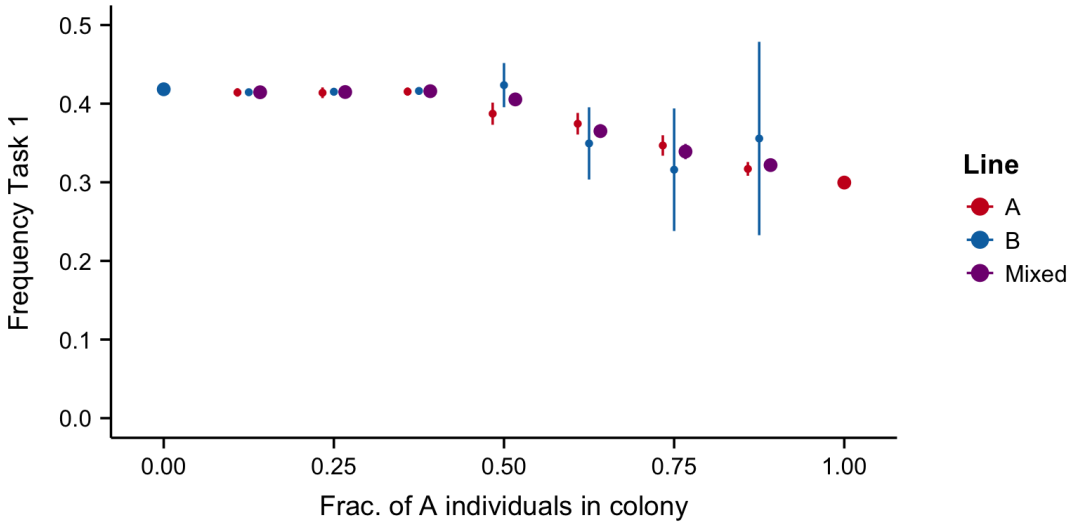

Figure 5: Simulation results for mixing of genetic lines when line B is inefficient. Parameters: $\alpha_j^A = 2, \alpha_j^B = 1$.

4 Varying task efficiency and mean threshold or threshold variance

We present two combinations of parameters that can capture the "negative" results in age and morphological mixing—where the two groups (young/old or workers/intercastes, respectively) differ in their mean behavior and mixing does not affect the behavior of each group. In Fig. 6, we varied the task efficiency (α) and the mean threshold (μ). In Fig. 7, we varied the task efficiency (α) and the threshold variance (σ). Both parameter combinations give rise to the desired pattern.

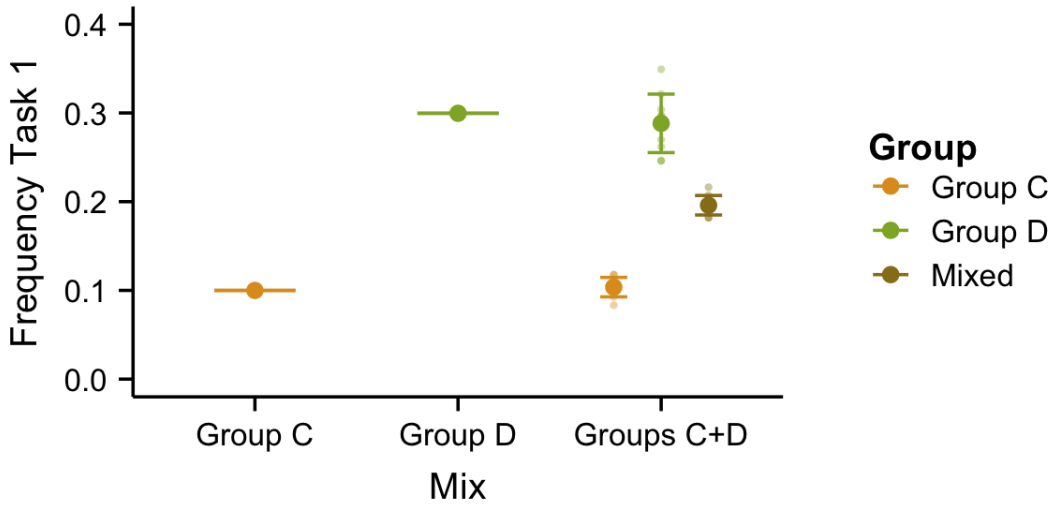

Figure 6: Simulation results for the mixing of two groups differing in task efficiency (α) and mean threshold (μ). Groups C and D represent demographic (young/old) or morphological (worker/intercaste) classes. Parameters: $\alpha_j^C = 6, \alpha_j^D = 2, \mu_j^C = 14, \mu_j^D = 10$.

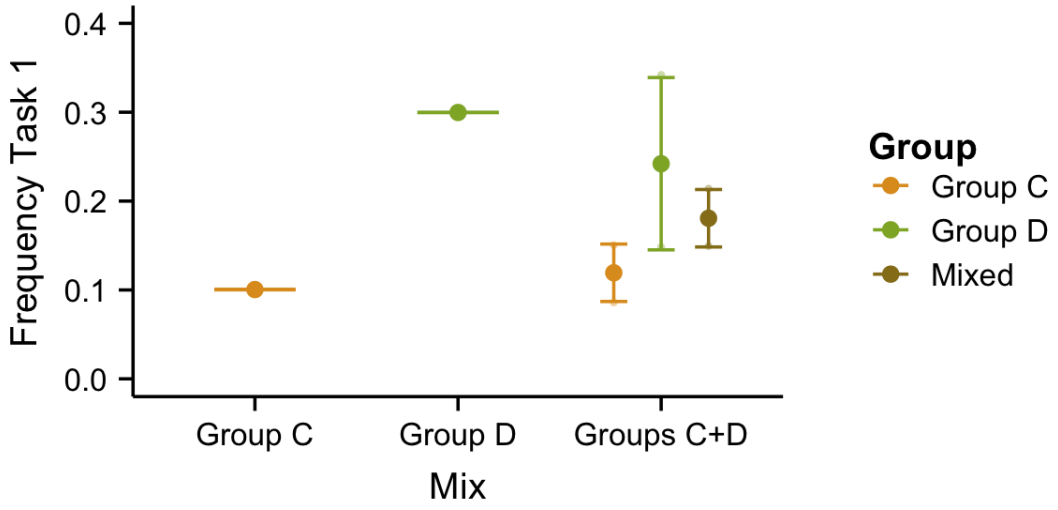

Figure 7: Simulation results for the mixing of two groups differing in task efficiency (α) and threshold variance (σ). Groups C and D represent demographic (young/old) or morphological (worker/intercaste) classes. Parameters: $\alpha_j^C = 6, \alpha_j^D = 2, \sigma_j^C = 0.1, \sigma_j^D = 0.5$.

5 Analytical model

To better understand our simulation results, we have developed and conducted a preliminary analysis of an analytical model with two different types of ants. The details of the model and the analysis are outlined in the Appendix; this section summarizes the most important takeaways.

The model considers n individuals and m tasks. The fractions of line A and B individuals are given by f and $1-f$, respectively. For example, $f=1$ corresponds to a pure A colony, $f=0.5$ to a 50:50 mixed colony, and $f=0$ to a pure B colony. The model captures the dynamics of 1) the number of line A and line B individuals performing task j at a given time, denoted $n^A_{j,t}$ and $n^B_{j,t}$ respectively, as well as 2) the stimuli associated with the two tasks. See Appendix A.1 for details.

5.1 Steady-state predictions 1: varying task efficiency and demand rate

We can analytically predict the task performance level in the steady state when only the task efficiency (α) and the demand rate (δ) are varied. Moreover, we can compute the condition under which the system is expected to reach a steady state (See Appendix A.2.1 for details).

Overall, our predictions perform well against the simulations. Figure 8 gives two illustrative comparisons. When all the ants in the colony are efficient, there is strong agreement between the predicted levels of task performance in the steady state (Fig. 8**a**). When some ants are inefficient (Fig. 8**b**), however, colonies violate the necessary condition for reaching a steady state; in this case, our steady-state predictions do not match the simulation results (as we would expect, since the system is not in equilibrium in the first place). A signature of this mismatch is that the stimuli run away (i.e., keep increasing over time).

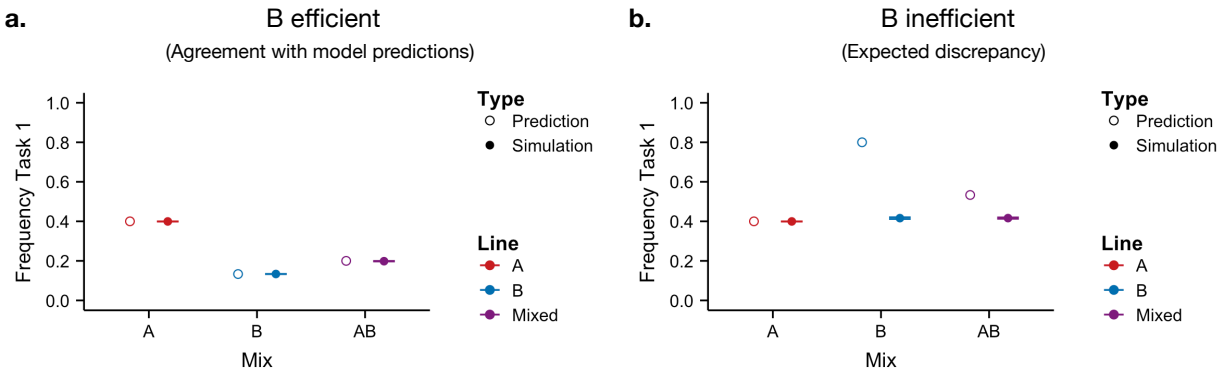

Figure 8: Comparison of simulation results and analytical predictions of steady states when line B is efficient (**a**, $\alpha^B_j=6$) and inefficient (**b**, $\alpha^B_j=1$). Line A is efficient in both **a** and **b**. Parameters: $\mu=10, \sigma=0, \eta=7, \delta=0.8$.

5.2 Steady-state predictions 2: symmetric mean thresholds

We can also predict the task performance level when the mean thresholds μ are varied symmetrically ($\mu^A_1=\mu^B_2$ and $\mu^A_2=\mu^B_1$) and all other parameters are the same between the two lines and tasks. Figure 9 compares two sets of simulation results and predictions. Our predictions show strong agreement with the simulations.

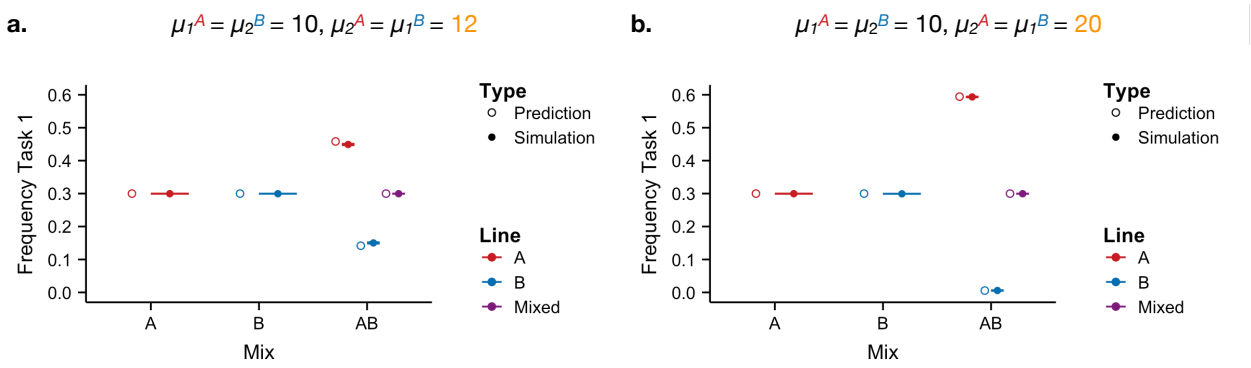

Figure 9: Comparison of simulation results and analytical predictions of steady states with symmetric mean thresholds. For both **a** and **b**: $\mu_1^A = \mu_2^B = 10$; for **a**: $\mu_1^B = \mu_2^A = 12$; for **b**: $\mu_1^B = \mu_2^A = 12$. Other parameters: $\mu = 10, \sigma = 0, \eta = 7, \delta = 0.6, \alpha = 2$.

5.3 Steady-state predictions 3: varying ratios of genetic lines

As an extension of Section 5.1, we can predict the steady-state task performance level with varied δ and α across colonies with different genetic ratios.

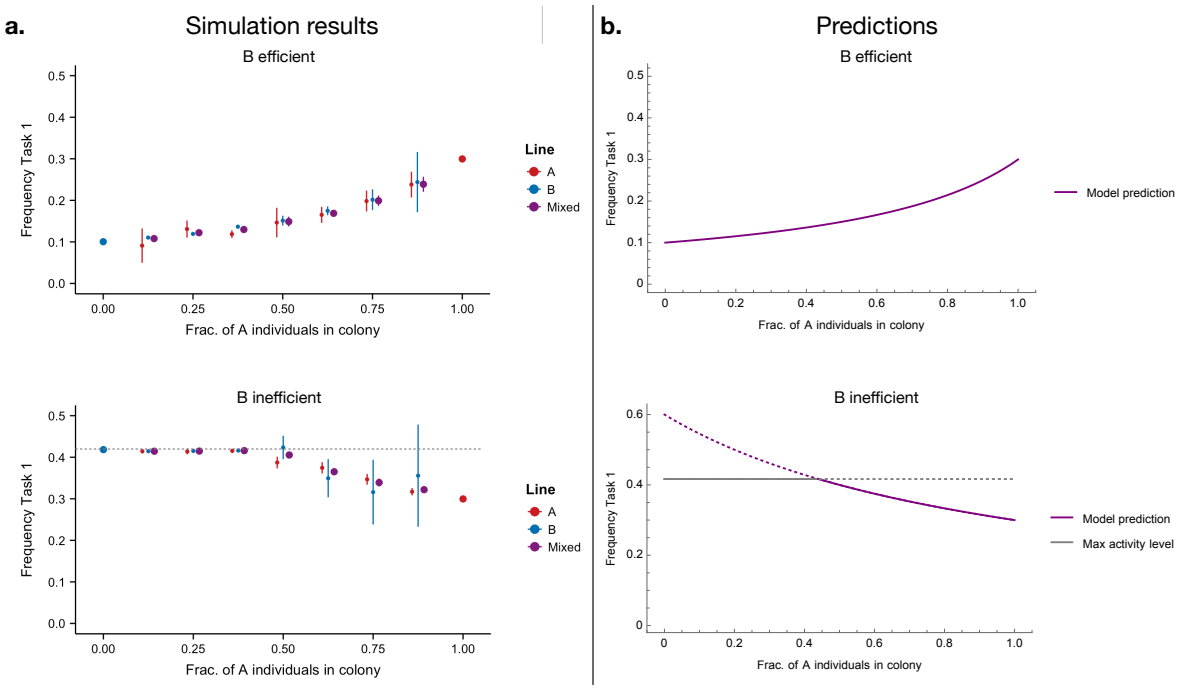

Figure 10: Comparison of simulation results (**a**) and analytical predictions (**b**) with varying ratios of line A and B ants. **Top row**: B ants are efficient ($\alpha_j^B = 6$). **Bottom row**: B ants are inefficient ($\alpha_j^B = 1$). The gray lines indicate the theoretically predicted maximal activity level for the given parameters (see Appendix A.2.1). Parameters: $\mu = 10, \delta = 0.6, \alpha_j^A = 2$.

Appendix

A Analytical model details

A.1 Model

To consider the dynamics of division of labor in mixed colonies, we extend the fixed threshold model in [1] to incorporate ants of two genetic lines, A and B.

The model considers n individuals and m tasks. Let f and $1-f$ be the fractions of genetic line A and B individuals in the colony, respectively. Each task j has an associated stimulus, $s_{j,t}$, at every time t, indicating the group-level demand for that task. We model the change in stimulus over discrete time as

$$s_{j,t+1} - s_{j,t} = \delta_j - \frac{\alpha_j^A n_{j,t}^A + \alpha_j^B n_{j,t}^B}{n}, \tag{1}$$

where δ_j is the task-specific demand rate; α_j^A and α_j^B are the task-specific performance efficiencies of lines A and B, respectively; and $n_{j,t}^A$ and $n_{j,t}^B$ are the numbers of line A and line B individuals performing task j and time t, respectively.

At each time step, inactive individuals are exposed to the task stimuli randomly until they either begin performing a task or have encountered all stimuli without landing on a task. Similar to [1], our computational model draws individual i's internal threshold θ_{ij} for task j from a normal distribution with mean μ_j and normalized standard deviation σ_j (each of which can be line- and/or task-specific). To gain analytical insight into the model, we make the simplifying assumption that $\sigma_j = 0$ for all tasks. In other words, *we assume that the line- and task-specific thresholds are given by the constant parameters, μ_j^A and μ_j^B.* With this assumption, the probabilities $P_{ij,t}^A$ and $P_{ij,t}^B$ that inactive individuals i of lines A and B begin to perform task j at time t can be written respectively as

$$P_{j,t}^A(s_{j,t}) = \frac{s_{j,t}^\eta}{s_{j,t}^\eta + (\mu_j^A)^\eta}, \quad P_{j,t}^B(s_{j,t}) = \frac{s_{j,t}^\eta}{s_{j,t}^\eta + (\mu_j^B)^\eta}. \tag{2}$$

The parameter η governs the steepness of the response threshold function as in the original model.

Finally, at time t, active individuals quit their tasks with a constant quit probability τ. In the case of two tasks ($m = 2$), the numbers of line A and line B individuals working on task j change according to the following:

$$\begin{aligned} n_{j,t+1}^A - n_{j,t}^A &= \frac{1}{2}\left[P_{j,t}^A(s_{j,t}) + (1 - P_{j',t}^A(s_{j',t}))P_{j,t}^A(s_{j,t})\right]\left(fn - (n_{j,t}^A + n_{j',t}^A)\right) - \tau n_{j,t}^A \\ n_{j,t+1}^B - n_{j,t}^B &= \frac{1}{2}\left[P_{j,t}^B(s_{j,t}) + (1 - P_{j',t}^B(s_{j',t}))P_{j,t}^B(s_{j,t})\right]\left((1-f)n - (n_{j,t}^B + n_{j',t}^B)\right) - \tau n_{j,t}^B \end{aligned} \tag{3}$$

for $(j, j') = (1, 2), (2, 1)$. The sums in square brackets capture the possible ways in which individuals can initiate task j: they can either encounter the stimulus for task j immediately and begin performing that task, or they can first encounter the stimulus for the other task j', decide not to perform that task, subsequently encounter the stimulus for task j, and begin performing task j.

The full model with two tasks ($m = 2$) consists of the six equations describing changes in s_1, s_2 (1) and $n_1^A, n_1^B, n_2^A, n_2^B$ (3).

A.2 Steady-state predictions

To understand how well the analtyical model captures the simulation results, we investigate the steady-state predictions of the analytical model for two tasks ($m = 2$).

A.2.1 A necessary condition for the existence of a biologically plausible equilibrium

In our computational model, the individuals essentially have a latency period of one time step between when they quit a task and recommence working. This means that, on average, only a fraction of the colony can be working at any given time.

To find this maximal activity level, let $X_t = (n^A_{1,t} + n^B_{1,t} + n^A_{2,t} + n^B_{2,t})/n$ be the fraction of active individuals in a colony at time t. Note that $0 \leq X_t \leq 1$. At time $t + 1$, a fraction τX_t of the colony is expected to be inactive. Therefore, at time $t + 1$,

$$(\text{fraction active}) + (\text{fraction inactive}) = X_{t+1} + \tau X_t \leq 1. \tag{4}$$

At steady state, $X_{t+1} = X_t = X^*$. By substitution, we obtain a necessary condition for a biologically plausible steady state to exist:

$$X^* \leq \frac{1}{1+\tau}. \tag{5}$$

For example, for $\tau = 0.2$ used in the simulations below, at most 83.33% of the individuals in a colony can be active at steady state. A similar condition for the theoretically possible maximum activity level at steady state has been noted in [2].

A.2.2 Pure colonies: 2 tasks, 1 line

For pure (A-only) colonies, we set $f = 1$ and $n^B_{j,t} = 0$ for all time t. Setting Eq. (1) to zero, we obtain

$$\frac{n^A_j}{n} = \frac{\delta_j}{\alpha^A_j} \tag{6}$$

as the fraction of A ants performing task j at steady state. Notably, the steady-state values of n^A_j are *independent* of the mean threshold (μ^A_j) or the quit probability (τ^A). This agrees our previous simulation results, where varying μ and τ by line did not change the mean task performance levels in pure colonies.

According to condition (5), this steady state is biologically possible only if

$$(X^* =) \frac{n^A_1}{n} + \frac{n^A_2}{n} = \frac{\delta_1}{\alpha^A_1} + \frac{\delta_2}{\alpha^A_2} \leq \frac{1}{1+\tau}. \tag{7}$$

If this condition is not met, then we would expect the stimuli to continue growing (i.e., the system will not reach a steady state).

A.2.3 Mixed colonies: 2 tasks, 2 lines, 50:50 mixes

We now consider the 50:50 mixes ($f = 0.5$), i.e., mixed colonies consisting of an equal number of A and B ants. Here we assume that the mean thresholds and the quit probabilities are identical for both tasks and lines ($\mu_1^A = \mu_2^A = \mu_1^B = \mu_2^B$ and $\tau^A = \tau^B$)[4], as we have done in the simulations with varied δ and α values. Setting Eqs. (1) and (3) equal to zero, we find the steady-state numbers of individuals performing task j as

$$n_j^A = n_j^B = n\left(\frac{\delta_j}{\alpha_j^A + \alpha_j^B}\right). \tag{8}$$

Alternatively, as fractions of each genetic type of individuals,

$$\frac{n_j^A}{(n/2)} = \frac{n_j^B}{(n/2)} = \frac{2\delta_j}{\alpha_j^A + \alpha_j^B}. \tag{9}$$

Applying condition (5), this state state exists only if

$$(X^* =) \sum_{j=1}^{2} \frac{n_j^A}{n} + \frac{n_j^B}{n} = \sum_{j=1}^{2} \frac{2\delta_j}{\alpha_j^A + \alpha_j^B} \leq \frac{1}{1+\tau}. \tag{10}$$

Again, if this condition is not met, then we would expect the stimuli to continue growing over time and for the ants to be working at max capacity.

A.2.4 Mixed colonies: 2 tasks, 2 lines, non-50:50 mixes

We now generalize to the case in which a fraction f of individuals in a mixed colony are of genetic line A. In the simplified case where $\mu_1^A = \mu_2^A = \mu_1^B = \mu_2^B$ and $\tau^A = \tau^B$, the steady-state fractions of individuals performing task j are

$$n_j^A = \frac{fn\delta_j}{f\alpha_j^A + (1-f)\alpha_j^B}, \quad n_j^B = \frac{(1-f)n\delta_j}{f\alpha_j^A + (1-f)\alpha_j^B}, \tag{11}$$

or, as fractions of the individuals of each genetic type (recall that there are fn individuals of type A and $(1-f)n$ individuals of type B),

$$\frac{n_j^A}{fn} = \frac{n_j^B}{(1-f)n} = \frac{\delta_j}{f\alpha_j^A + (1-f)\alpha_j^B} \left(= \frac{n_j^A + n_j^B}{n} \right). \tag{12}$$

The last equality highlights the fact that the fraction of individuals *of each type* performing task j is identical to the fraction *of the whole colony* performing that task. As expected, the expressions (12) reduce to (9) when $f = 0.5$ (50:50 mixes) and to (6) when $f = 1$ (pure A colonies). Again, we would expect to see this equilibrium only when condition (5) is satisfied.

From these results, we would expect the steady-state fraction of task j performance frequency (which corresponds to (12)) to depend *nonlinearly* on the fraction of A individuals (f).

[4]The parameters μ and τ do not explicitly appear in (9) when we assume that the mean thresholds are identical for all individuals and both tasks. However, based on the Eqs. (3), we expect the general form of steady state fractions of active individuals to be explicit functions of μ_j^A and μ_j^B as well as τ^A and τ^B. The steady states can be computed numerically for the case when these parameters vary, but the analytical expression is too complicated to write down.

A.2.5 Mixed colonies: 2 tasks, 2 lines, 50:50 mixes, symmetric mean thresholds

So far we have assumed that the mean thresholds μ_j^A and μ_j^B were identically for both lines and tasks ($\mu_1^A = \mu_2^A = \mu_1^B = \mu_2^B$). While the system of equations can be solved numerically even when we vary μ, the steady-state expressions quickly become too complicated to write down.

In the following special case, however, we can express the equilibrium values exactly. Assume that

- 1) the task efficiencies are the same for both lines and tasks ($\alpha_1^A = \alpha_2^A = \alpha_1^B = \alpha_2^B = \alpha$);
- 2) the quit probabilities are the same for both tasks ($\tau^A = \tau^B = \tau$); and
- 3) the task demand rates are the same for both tasks ($\delta_1 = \delta_2 = \delta$); 4) the task thresholds are "symmetric": $\mu_1^A = \mu_2^B = a$ and $\mu_2^A = \mu_1^B = b$.

The symmetry of the parameters means that the dynamics of the stimuli are identical. Therefore, at steady state, the stimulus levels should be equal ($s_1 = s_2 = s$). Moreover, the number of A ants performing task 1 should be identical to that of B ants performing task 2 ($n_1^A = n_2^B$) and the number of B ants performing task 1 should be identical to that of A ants performing task 2 ($n_1^B = n_2^A$).

Taking advantage of this symmetry, we can write down the steady-state stimulus level s ($= s_1 = s_2$) as

$$s^* = \left[\frac{1}{2}\left(-(a^\eta + b^\eta) \pm \sqrt{(a^\eta + b^\eta)^2 + (a^\eta b^\eta) \cdot \frac{8\delta\tau}{\alpha - 2\delta(1+\tau)}}\right)\right]^{\frac{1}{\eta}}. \tag{13}$$

The corresponding steady-state fractions of A and B ants performing tasks 1 and 2 are

$$\frac{n_1^A}{(n/2)} = \frac{n_2^B}{(n/2)} = \frac{1}{\tau}\left(\frac{(s^*)^\eta}{(s^*)^\eta + a^\eta}\right)\left[2 - \frac{(s^*)^\eta}{(s^*)^\eta + b^\eta}\right]\left(\frac{1}{2} - \frac{\delta}{\alpha}\right) \tag{14}$$

$$\frac{n_2^A}{(n/2)} = \frac{n_1^B}{(n/2)} = \frac{1}{\tau}\left(\frac{(s^*)^\eta}{(s^*)^\eta + b^\eta}\right)\left[2 - \frac{(s^*)^\eta}{(s^*)^\eta + a^\eta}\right]\left(\frac{1}{2} - \frac{\delta}{\alpha}\right) \tag{15}$$

When $a = b$ (i.e., when all μ's are the same), (14) and (15) reduce to the steady-state values predicted in (9).

A.3 Downward vs. upward contagion

One question that was raised during our previous discussion was whether varying both the task efficiency α and the demand rate δ would capture the difference in the directions of convergence (downward or upward) when the larvae differed. In Section 2, we presented simulation results that suggested that upward contagions only occur when some of the ants are inefficient and therefore the colony cannot maintain the stimuli at a steady level. Here we show analytically that, *if the system reaches its steady state (i.e., condition* (5) *is satisfied), then varying* ***only*** *the demand rate (δ) and task efficiency (α) can result in a downward contagion but not an upward contagion.*

If we only vary δ and α, then the mean thresholds and the quit probabilities are identical across tasks and lines. So we can directly apply the steady-state fractions of active individuals computed in Eqs. (6) and (9). The behavioral contagion is "downward" if

$$\frac{1}{2}\left(\frac{\delta_j}{\alpha_j^A} + \frac{\delta_j}{\alpha_j^B}\right) > \frac{2\delta_j}{\alpha_j^A + \alpha_j^B} \tag{16}$$

and "upward" if the inequality is reversed (the schematic in Fig. 11 should help).

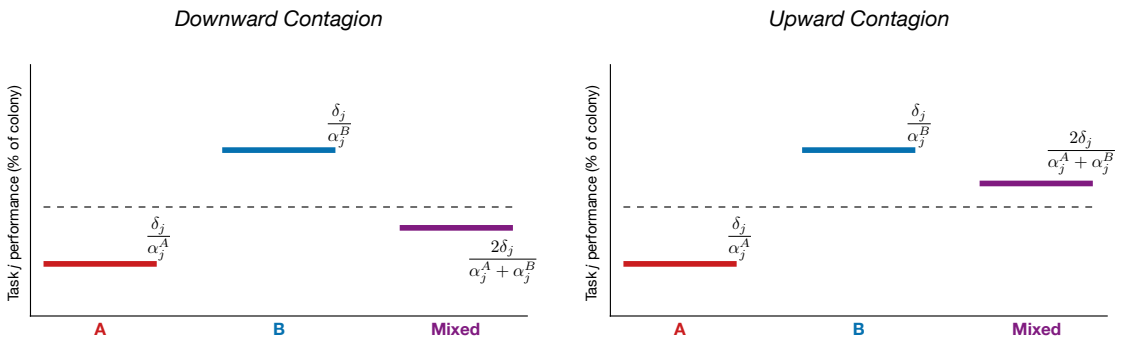

Figure 11: A schematic representing the two contagion patterns of our interest. The task j performance (%) values for the mixed colonies assume that the mean thresholds and the quit probabilities are identical for both lines and both tasks ($\mu_1^A = \mu_2^A = \mu_1^B = \mu_2^B$ and $\tau^A = \tau^B$).

By manipulating the inequality (16), however, we see that the LHS is always at least as large as the RHS:

$$\frac{1}{2}\left(\frac{\delta_j}{\alpha_j^A} + \frac{\delta_j}{\alpha_j^B}\right) - \frac{2\delta_j}{\alpha_j^A + \alpha_j^B} = \frac{\delta_j}{2}\left(\frac{(\alpha_j^A - \alpha_j^B)^2}{\alpha_j^A \alpha_j^B (\alpha_j^A + \alpha_j^B)}\right) \geq 0 \tag{17}$$

The equality holds if and only if $\alpha_j^A = \alpha_j^B$, in which case the ants are indistinguishable with respect to task j (the three lines take the same value for task j). If $\alpha_j^A \neq \alpha_j^B$, then only a downward contagion is possible under our assumptions.

Upward contagion is still possible if we relax some of our assumptions. For example,

- when the mean threshold (μ) is varied in addition to the task efficiency (α), or
- when some ants are too inefficient to maintain the stimuli at constant levels (i.e., reach steady state).

References

[1] Y. Ulrich, J. Saragosti, C. K. Tokita, C. E. Tarnita, D. J. C. Kronauer, "Fitness benefits and emergent division of labour at the onset of group living," *Nature*, vol. 560, pp. 635-638, Aug. 2018.

[2] J. Gautrais, G. Theraulaz, J. L. Deneubourg, C. Anderson, "Emergent polyethism as a consequence of increased colony size in insect societies," *Journal of Theoretical Biology*, vol. 215, pp. 363–373, Apr. 2002.